Journal of Alloys and Compounds 509 (2011) 3541–3546

Contents lists available at ScienceDirect

Journal of Alloys and Compounds

journal homepage: www.elsevier.com/locate/jallcom

# Study of post annealing influence on structural, chemical and electrical properties of ZTO thin films

Vipin Kumar Jain[a,*], Praveen Kumar[b], Mahesh Kumar[b], Praveen Jain[c], Deepika Bhandari[d], Y.K. Vijay[a]

[a] Thin film & Membrane Science Laboratory, University of Rajasthan, Jaipur 302004, India
[b] Surface Physics and Nanostructures Group, National Physical Laboratory, New Delhi 110012, India
[c] Department of Physics, Indian Institute of Technology, Roorki 247667, India
[d] Department of Physics, S.S. Jain Subodh (P.G.) College, Jaipur 302004, India

ARTICLE INFO

*Article history:*
Received 8 June 2010
Received in revised form 11 October 2010
Accepted 21 October 2010
Available online 2 December 2010

*Keywords:*
ZTO thin film
Flash evaporation
XRD
AFM
XPS
Electrical resistivity

ABSTRACT

Zinc–Tin-Oxide (ZTO) thin films were deposited on glass substrate with varying concentrations ($ZnO:SnO_2$; 100:0, 90:10, 70:30 and 50:50 wt.%) at room temperature by flash evaporation technique. These deposited ZTO films were annealed at 450 °C in vacuum. These films were characterized to study the effect of annealing and addition of $SnO_2$ concentration on the structural, chemical and electrical properties. The XRD analysis indicates that crystallization of the ZTO films strongly depends on the concentration of $SnO_2$ and post annealing where annealed films showed polycrystalline nature. Atomic force microscopy (AFM) images manifest the surface morphology of these ZTO thin films. The XPS core level spectra of Zn(2p), O(1s) and Sn(3d) have been deconvoluted into their Gaussian component to evaluate the chemical changes, while valence band spectra reveal the electronic structures of these films. A small shift in Zn(2p) and Sn(3d) core level towards higher binding energy and O(1s) core level towards lower binding energy have been observed. The minimum electrical resistivity ($\rho \approx 3.69 \times 10^{-2}$ Ω-cm), maximum carrier concentration ($n \approx 3.26 \times 10^{19}$ cm$^{-3}$) and Hall mobility ($\mu \approx 5.2$ cm$^2$ v$^{-1}$ s$^{-1}$) were obtained for as-prepared ZTO (50:50) film thereafter move towards lowest resistivity ($\rho \approx 1.12 \times 10^{-3}$ Ω-cm), highest carrier concentration ($n \approx 2.96 \times 10^{20}$ cm$^{-3}$) and mobility ($\mu \approx 18.8$ cm$^2$ v$^{-1}$ s$^{-1}$) for annealed ZTO (50:50) thin film.

© 2010 Elsevier B.V. All rights reserved.

## 1. Introduction

TCO semiconductors such as indium tin oxide (ITO), $SnO_2$, ZnO have been studied and used technologically for more than 50 years because of their good optical and electrical properties in combination with their large band gap ($E_g > 3$ eV), abundance in nature and absence of toxicity [1–3]. These TCO films are used as transparent electrodes of flat-panel devices, gas sensors, solar cell, light emitting diode (LED), etc. [4–6]. Although these thin films have been proved to have relatively good optical and electrical conductivity but they are limited in their application due to chemical and/or thermal instabilities in certain environments. To obtain suitable, improved TCO coatings for specialized applications, new materials have been studied in recent years [7–10]. Apart from other TCO thin films, ZTO thin films show their promising applications as an alternative TCO material due to their low cost (as the constituents ZnO and $SnO_2$ are much cheaper) and their properties which can be tailored to have the advantage of good thermal stabilities under the reducing atmosphere. Ko et al. [11] investigated the effect of ZnO on the electrical and structural properties of $SnO_2$ films. Further, the efficiency and performance of the device depend on the various parameters like percentage of dopant, pre-annealing rate, deposition rate, and post annealing treatment, electrical, and optical properties of the TCO materials used in their construction.

The present work deals with study of the structural, chemical, and electrical properties of ZTO thin films as a function of $SnO_2$ concentration, ranging from 0 to 50 wt.%. The thin films are prepared by flash evaporation technique [12]. Further, an effort has also been made to study the effect of post annealing on these properties.

### 2. Experimental detail

ZTO thin films were deposited on glass substrates by Flash evaporation technique at a pressure of $10^{-6}$ Torr. High purity ZnO (99.99%) and $SnO_2$ (99.9%) powders at different concentrations (100:0, 90:10, 70:30 and 50:50 wt.%) were mixed with the help of stainless steel balls at 250 rpm for 1 h using ball milling (Retsch-TM100, Germany). Fig. 1 is the schematic diagram of the evaporation technique adopted in this study in which a mixture of the components in powder form is fed in to a resistively heated tantalum or tungsten boat by electrophonically agitating the feed chute for the instantaneous evaporation of the powdered material. The temperature of the boat was maintained at a temperature sufficiently higher than the melting point of the evaporants. This high temperature ensures instantaneous vaporization of the material and also imparts sufficient kinetic energy to the particles in the vapor phase.

* Corresponding author. Tel.: +91 9828117678; fax: +91 1412702457.
*E-mail address:* vipinjain7678@gmail.com (V.K. Jain).

0925-8388/$ – see front matter © 2010 Elsevier B.V. All rights reserved.
doi:10.1016/j.jallcom.2010.10.212

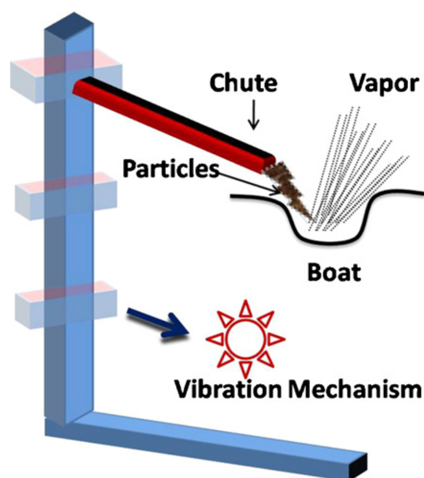


**Fig. 1.** Schematic diagram of flash evaporation technique.

Then vapors were condensed to form a film on a nearby substrate, ensuring the stoichiometry of the films. The temperature of the substrate (room temperature) was low enough to prevent the re-evaporation of any condensing component. The spacing between target and substrate was fixed at 10 cm. The thickness of the prepared films was measured by a quartz crystal thickness monitor. The thickness of all the films was observed in the range 1000 ± 25 Å. Deposition conditions were carefully maintained during the growth of ZTO films. The as-prepared films were studied in terms of structural, chemical and electrical properties. The crystalline phase of films was identified using X-ray diffractometer (Bruker AXS) with monochromatic Cu-$K_\alpha$ radiation (0.154 nm). Surface morphology of the films was investigated by AFM (Digital Instruments NanoScope IIIa). The chemical composition and bonding states of the ZTO thin films were characterized by X-ray photoelectron spectroscopy (Perkin Elmer-1257) using Mg-$K_\alpha$ (1.2536 keV) radiation at a base pressure of $5 \times 10^{-10}$ Torr. The electrical resistivity, carrier concentration, and Hall mobility of the films were determined by Hall measurements using the four-probe van der Pauw technique.

Further, these ZTO thin films were annealed in vacuum at the temperature of 450 °C for 1 h. The heating rate was kept at 10 °C/min. The annealed films were also characterized by XRD, AFM, and XPS measurements. Electrical measurements were taken with the same instruments mentioned above.

## 3. Results and discussion

ZTO thin films at different concentrations (100:0, 90:10, 70:30 and 50:50 wt.%) were prepared by flash evaporation technique at pressure of $10^{-6}$ Torr using vacuum coating unit. The films were characterized by studying the structural, chemical, and electrical properties.

### 3.1. X-ray diffraction (XRD) analysis

The as-prepared and annealed ZTO thin films were characterized by X-ray diffraction (XRD) to see the nature of films. Fig. 2(a) and (b) displays the XRD patterns of as-prepared and annealed films, respectively. Fig. 2(a) shows the amorphous nature of pure ZnO or ZTO (100:0) and ZTO (90:10) thin films. However, two poor peaks indexed (2 2 0) and (2 2 1) were started appearing near 2$\theta$ angle of 30.5° and 32.2°, respectively, in ZTO (70:30) film indicating the polycrystalline cubic structure. The intensity of these peaks was increased and a very small new cubic (3 2 2) peak was observed near 44.9° in ZTO (50:50) thin film. The lattice constant for these peaks was calculated by Powder-X software and its value is obtained to be $a$ = 0.831 nm which is very close to that of the cubic $Zn_2SnO_4$ ($a$ = 0.865 nm, JCPDS file 24-1470). These new peaks might be due to formation of compounds like $(ZnO)_{1-x}(SnO_2)_x$, $(Zn_2SnO_4)_{1-X}(ZnO)_X$ and $(ZnSnO_3)_{1-X}(SnO_2)_X$, etc. as also reported earlier [13,14]. The amorphous phase completely disappeared after annealing as can be seen in Fig. 2(b). The ZTO thin films became polycrystalline where crystalline peaks of ZTO (100:0) film were well matched with the vertical lines of hexagonal ZnO reference peaks ($a$ = 0.324 nm and $c$ = 0.520 nm, JCPDS file 03-0888) having prominent orientation (1 0 1) near 42.3° with a weak peak (0 0 2). Intensity of ZnO peaks gradually decreased with increasing the concentration of $SnO_2$ and cubic (2 2 0) and (2 2 1) peaks were observed at the same position of the as-prepared ZTO films but became stronger after annealing. It was noticeable that small addition of $SnO_2$ into ZnO enhance the intensity of cubic (2 2 0) and (2 2 1) peaks in accordance with as-prepared ZTO thin films. The linear variation of intensity ratio of cubic (2 2 0) and hexagonal (1 0 1) orientation and grain size of annealed ZTO thin films with concentration of $SnO_2$ is illustrated in Fig. 3. This indicates that a preferential crystal growth towards the (2 2 0) orientation took place after increasing the concentration of $SnO_2$.

The grain size of ZTO crystallites was estimated in the direction (2 2 0) using the Debye–Scherrer equation [15]

$$D = \frac{0.89\lambda}{\beta \cos\theta}$$

where $D$ is the crystal size, $\lambda$ is the wavelength of the X-ray, $\beta$ is the difference between measured full width at half maximum (FWHM) of (2 2 0) peak and the unbroadened FWHM of single crystal, which was taken as 0.047°. The grain size of as-prepared ZTO (70:30) and ZTO (50:50) film was also estimated to be ≈15 nm and ≈20 nm, respectively. The estimated

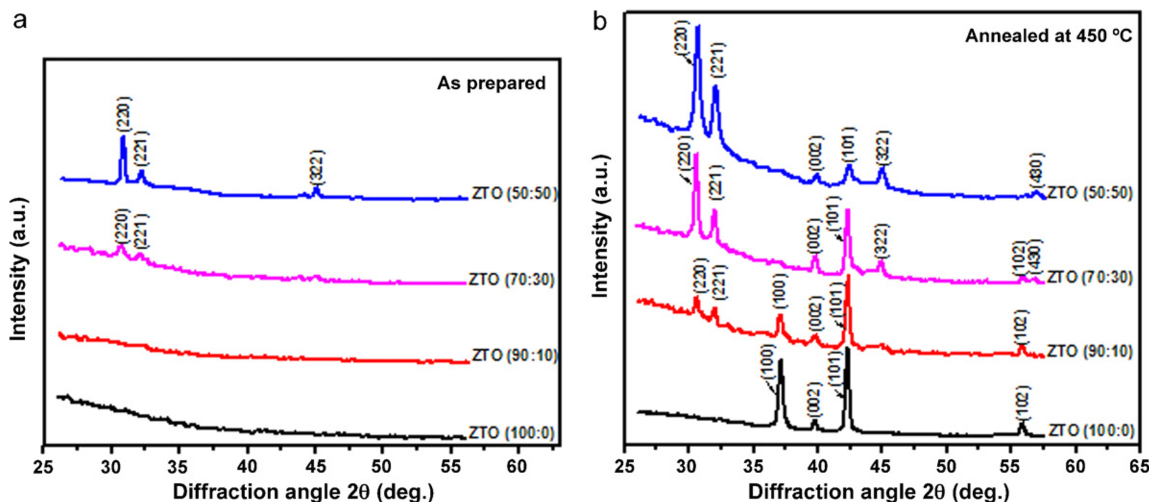


**Fig. 2.** XRD profile of (a) as-prepared and (b) annealed ZTO thin films.

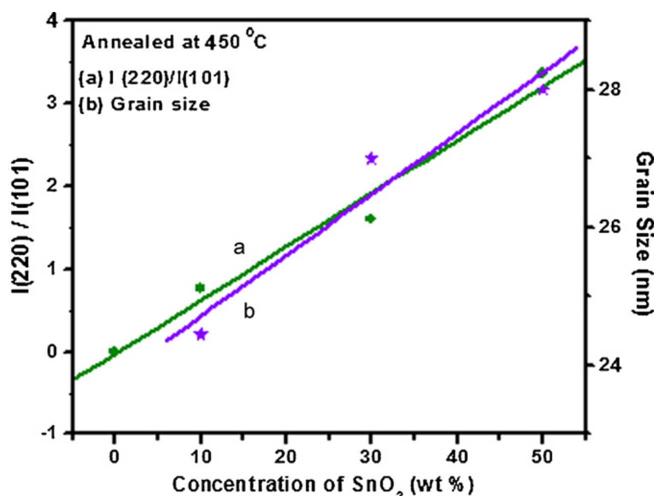


**Fig. 3.** The ratio of (2 2 0) and (1 0 1) intensities and grain size with the varying concentration of $SnO_2$ of annealed film.

grain size of the annealed ZTO films is shown in Fig. 3 which is enhanced from ≈24 nm to ≈28 nm with the increase of $SnO_2$ concentration from 10 to 50 wt.%. The increment in grain size can be attributed to improvement of crystallinity with increasing concentration of $SnO_2$ and post annealing. It was found that grain size enhanced with the post annealing as well as with improving concentration of $SnO_2$ due to which surface adatom mobility of the species increases leading to coalition of smaller grains.

### 3.2. Atomic force microscopy (AFM) studies

The surface morphology of the films has been studied by atomic force microscopy (AFM). Fig. 4 shows the surface morphology of as-prepared and annealed ZTO (50:50 wt.%) thin films as a specimen. The apparent growth of surface features in both types of ZTO films is evident from two dimensional AFM images. The AFM data showed that the ZTO thin films were homogeneous and uniform with regard to surface topography and thickness. The film deposited at room temperature revealed that the film is composed of roughly spherical grains of varying sizes which seem to be arranged in arrays. The average grain size calculated was 44 nm. The grain size increased after annealing. This trend is in agreement with XRD findings that particle size enhances after annealing. There can be a difference between the particle sizes obtained from XRD and AFM as AFM gives a surface scan whereas X-ray penetrates the material.

### 3.3. X-ray photoelectron spectroscopy (XPS) studies

XPS study has been carried out to study the chemical bonding of these as-prepared and annealed ZTO films. Fig. 5 shows the Gaussian deconvoluted XPS core level spectra of Zn($2p_{3/2}$), O(1s) and Sn($3d_{5/2}$) for the as-prepared while Fig. 6 shows the same for annealed ZTO films. The binding energies were calibrated by taking the C(1s) peak at 284.6 eV. The binding energy of Zn($2p_{3/2}$), O(1s) and Sn($3d_{5/2}$) exhibit peaks at 1021.8 ± 0.3 eV, 531.6 ± 0.3 eV and 486.2 ± 0.3 eV, respectively. These core level spectra have been deconvoluted into their Gaussian components by considering position and FWHM according to the literature [16]. Zn(2p) core level spectra have been deconvoluted into two main Gaussian components, one at 1021.9 eV and latter at 1023.5 eV can be attributed to the Zn–O and Zn–O–Sn related contribution, respectively. In the same fashion, Sn(3d) core level spectra have been deconvoluted into three Gaussian components at 484.3 eV, 486.2 eV and 487.2 eV correspond to metallic Sn, Sn(+4) state and Sn(+2) state, respectively [17]. The intensity of these peaks increased with increase in Sn content. The presence of SnO derived components in the Sn $3d_{5/2}$ spectra should be attributed to lattice oxygen deficiency and reduced oxygen concentration at the surface, becoming more prominent after annealing, which results in the enhancement of intensity ratio corresponding to peak of SnO and $SnO_2$ after annealing. The XPS peaks in the regions of O(1s) measured at two different conditions exhibit the existence of oxygen in different environment in ZTO films. The peaks observed under as-prepared condition at around 530.5 eV, 531.5 eV and 532.5 eV suggested the existence of three different environments while the peak observed at ∼530.5 eV as well as ∼532.5 eV shrink and ∼531.5 eV grow under annealed condition. The peak at ∼532.5 eV may be attributed to the oxygen of free hydroxyl groups which is possibly due to environmental moisture trapped in the film surface [18]. The peak at around 530.5 eV may be assigned as due to oxygen in lattice crystal [19] and other peak at around 531.5 eV might be due to $O^{2-}$ in an oxygen deficient region [20]. Further, it was observed that Zn(2p) and Sn(3d) peak slightly shift towards the higher binding energy but O(1s) peak shifts towards the lower binding energy as percentage composition of $SnO_2$ increased. This behavior is an indicator for limiting the formation of Zn–O–Sn linkage and favoring formation of mixed oxides of ZnO and $SnO_2$ as also reported [18].

Fig. 7(a) and (b) shows the XPS valence band spectra of as-prepared and annealed samples respectively, obtained at normal emission (0°) in VB region (−5 eV to 10 eV). It was observed from Fig. 7(a) that valence band maxima lies after the Fermi level at ∼1.8 eV for as-prepared ZTO (100:0) film and shows the band gap of ∼3.6 eV. It was perceptible that addition of $SnO_2$ into ZnO shifts valance band maxima towards lower binding energy with presence of some states near the Fermi level which results the valence band maxima come near the Fermi level at ∼1.65 eV for as-prepared ZTO (50:50) film and shows the band gap of ∼3.3 eV. This indicated the transition of films towards more conducting nature.

Fig. 7(b) shows the similar trend for the reduction of the band gap with increase in $SnO_2$ concentration in annealed ZTO films. Figure also demonstrates an interesting dependence on temperature of these films, which manifest the decrease in the band gap after annealing as compared to the as-prepared samples. The valence band maxima move towards the Fermi level at ∼1.55 eV for annealed ZTO (50:50) film and show the band gap of ∼3.1 eV.

### 3.4. Electrical properties

The electrical resistivity, carrier concentration and Hall mobility of both types of ZTO thin films (as-prepared and annealed) deposited at different concentration of $SnO_2$ was investigated. Fig. 8 summarizes electrical resistivity results of as-prepared and annealed ZTO thin films. It can be noted from the figure that the resistivity of as-prepared ZTO thin film decreases with the increasing concentration of $SnO_2$.

The decrease in resistivity ($\rho$) with the increasing concentration of tin can be attributed to the increase in the carrier concentration ($n$) and the mobility ($\mu$) of the charge carriers as resistivity is given by

$$\rho = \frac{1}{\sigma} = \frac{1}{qn\mu},$$

where $\sigma$ is the conductivity of the film and $q$ is the charge of the carriers.

In ZTO thin films, the tin atoms may diffuse into ZnO matrix. Due to difference in their grain sizes, diffusion of tin atoms in ZnO matrix

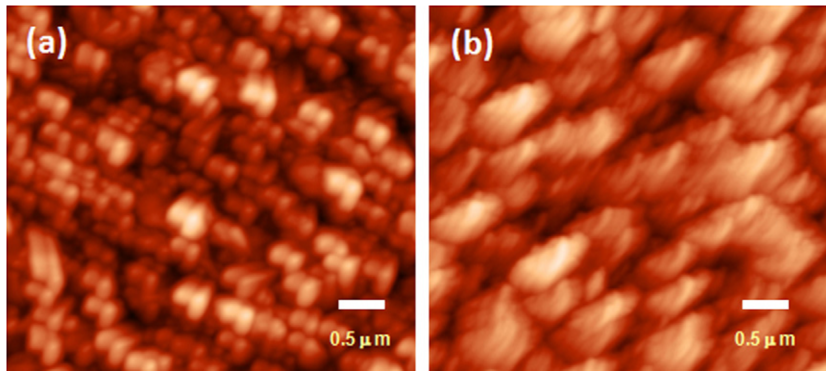


**Fig. 4.** Atomic force micrograph of (a) as-prepared (b) annealed ZTO (50:50 wt.%) thin films.

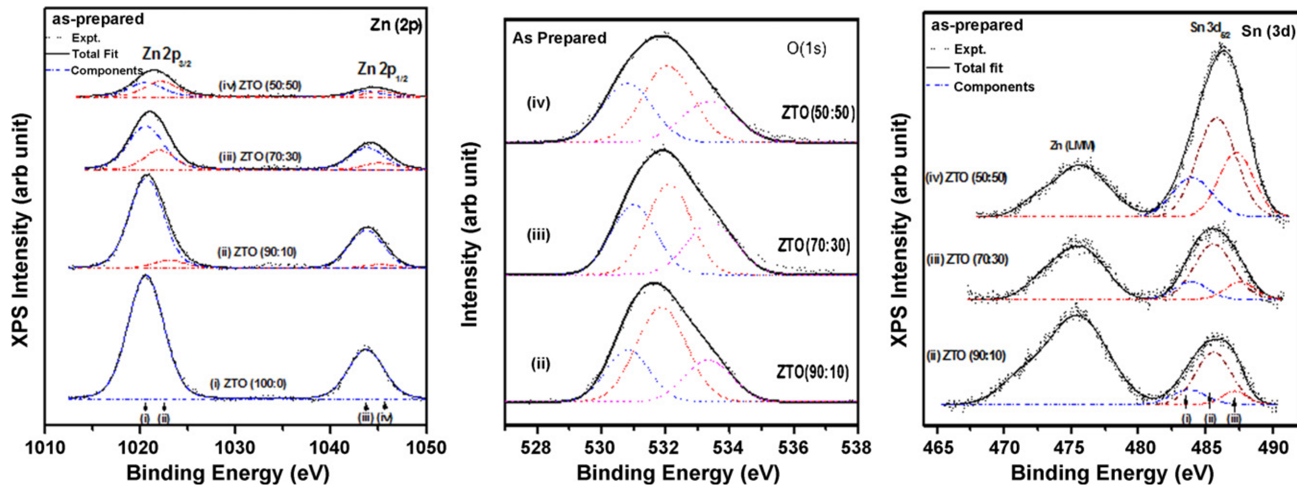


**Fig. 5.** Peak fitting results of Zn $2p_{3/2}$, O1s and Sn $3d_{5/2}$ narrow XPS spectra of as-prepared ZTO thin films with varying concentration ($ZnO:SnO_2$ = (i) 100:0, (ii) 90:10, (iii) 70:30, (iv) 50:50 wt.%).

causes an increase in free interstitial lattice spaces. The mobility of valance electrons is increased in these free spaces and from above equation, increases in mobility causes the decrease in resistivity (or increase in electrical conductivity). Being less electronegative than zinc (Zn), tin (Sn) atoms behave as donors and enhance the carrier concentration. Further, the oxygen vacancies also play a very important role in the electronic properties of ZTO thin films. Oxygen vacancies like defects are the primary source of charge carriers. The usual description of oxygen-vacancy doping in crystalline ZTO thin film using Kreoger–Vink notation is given as

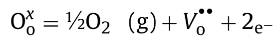

$$O_o^x = ½O_2 \quad (g) + V_o^{\bullet\bullet} + 2_{e^-}$$

which indicates that oxygen on the oxygen sub-lattice ($O_o{}^x$) lost as oxygen gas ($O_2$) creates a doubly charge oxygen vacancy ($V_o^{\bullet\bullet}$) and two free electrons [21,22], hence increases the concentration of charge carriers. As number of charge carrier increases, resistivity decreases.

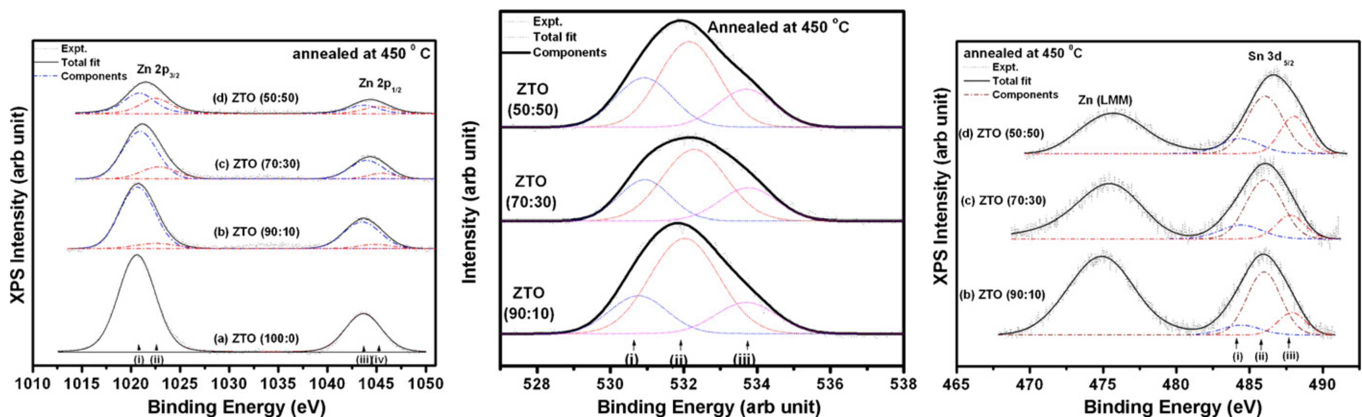


**Fig. 6.** Peak fitting results of Zn $2p_{3/2}$ and Sn $3d_{5/2}$ narrow XPS spectra of annealed ZTO thin films with varying concentration ($ZnO:SnO_2$ = (i) 100:0, (ii) 90:10, (iii) 70:30, (iv) 50:50 wt.%).

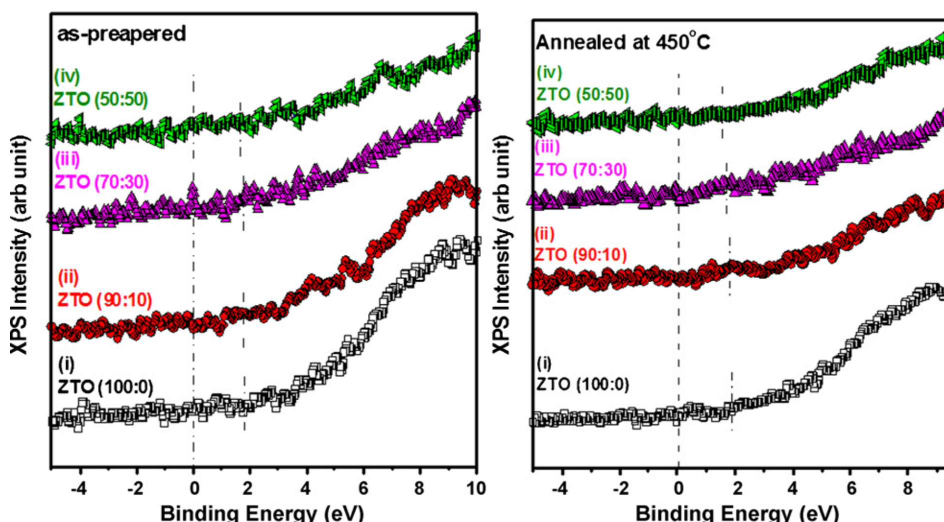


**Fig. 7.** XPS valance band spectra of (a) as-prepared and (b) annealed ZTO thin films with varying concentration ($ZnO:SnO_2$ = (i) 100:0, (ii) 90:10, (iii) 70:30, (iv) 50:50 wt.%).

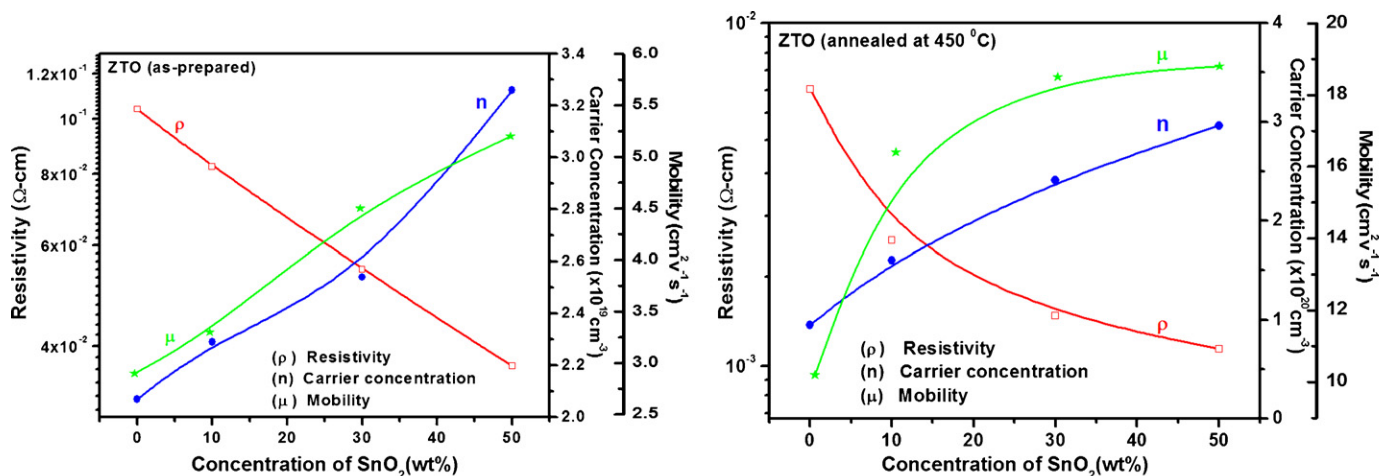


**Fig. 8.** The electrical resistivity, carrier concentration and Hall mobility of (a) as-prepared and (b) annealed ZTO thin films with varying concentration ($ZnO:SnO_2$ = (i) 100:0, (ii) 90:10, (iii) 70:30, (iv) 50:50 wt.%).

After annealing in vacuum at 450 °C, the resistivity of ZTO film is found to decrease remarkably as compared to as-prepared film. Its value reaches to the order of $\sim 10^{-3}\ \Omega$-cm. This may be due to further increase in mobility and carrier concentration on heat treatment given to the films. The annealing process causes a greater possibility of diffusion of Sn atom from grain boundaries and interstitial lattice locations to regular ZnO lattice locations [23]. After annealing the grain growth results in less grain boundary and, consequently, there is less grain-boundary scattering and thus the mobility of the charge carriers enhanced. On vacuum annealing, oxygen vacancies further enhance and create more free electrons and result in to an increase in carrier concentration. After annealing, tin atoms are activated and behave as effective donors. Hence, the number of free electrons in the annealed film increases drastically. The values of so-obtained electrical resistivity of both types of films are listed in Table 1. The minimum electrical resistivity ($\rho \approx 3.69 \times 10^{-2}\ \Omega$-cm), maximum carrier concentration ($n \approx 3.26 \times 10^{19}\ cm^{-3}$) and mobility ($\mu \approx 5.2\ cm^2\ v^{-1}\ s^{-1}$) were obtained for as-prepared ZTO (50:50) film. For annealed ZTO (50:50) thin films, the corresponding values obtained were lowest resistivity ($\rho \approx 1.12 \times 10^{-3}\ \Omega$-cm), highest carrier concentration ($n \approx 2.96 \times 10^{20}\ cm^{-3}$) and mobility ($\mu \approx 18.8\ cm^2\ v^{-1}\ s^{-1}$).

## 4. Conclusions

In the present study, the structural, chemical and electrical properties of cost effective ZTO thin films with varying concentrations have been studied. Effect of annealing has also been studied. It was observed that crystalline nature of ZTO thin films was shifted from hexagonal structure to cubic structure with increasing concentration of $SnO_2$. The XRD and AFM results are evidences for enhancement of the size of the spherical grains after annealing. XPS evaluate the chemical nature of as prepared as well as annealed films. The XPS results revealed that in ZTO films, Sn is present in three states {metallic Sn, Sn(+2) and Sn(+4)}, while Zn is present in two states {Zn(+2) and Zn(+4)} and O is also present in three states. The presence of SnO derived components in the Sn $3d_{5/2}$ spectra should be attributed to lattice oxygen deficiency and reduced oxygen concentration at the surface which suggest the reduction in resistivity. The shifting of Zn, Sn and O core level peak limit the formation of Zn–O–Sn linkage and favoring formation of mixed oxides of ZnO and $SnO_2$. A drastic decrease in electrical resistivity was observed with the increasing concentration of $SnO_2$ and after annealing. This may be attributed to increase in carrier concentration and mobility due to diffusion process, oxygen vacancy, less grain-boundary scattering, etc.

**Table 1**
Electrical resistivity, carrier concentration and Hall mobility of as-prepared and annealed ZTO thin films.

| Sample | As-prepared | | | Annealed at 450 °C | | |
|---|---|---|---|---|---|---|
| | $\rho$ (Ω-cm) | $n$ ($\times 10^{19}$ cm$^{-3}$) | $\mu$ (cm$^2$ v$^{-1}$ s$^{-1}$) | $\rho$ (Ω-cm) | $n$ ($\times 10^{20}$ cm$^{-3}$) | $\mu$ (cm$^2$ v$^{-1}$ s$^{-1}$) |
| ZTO (100:0) | $10.4 \times 10^{-2}$ | 2.07 | 2.9 | $6.41 \times 10^{-3}$ | 0.95 | 10.2 |
| ZTO (90:10) | $8.25 \times 10^{-2}$ | 2.29 | 3.3 | $2.32 \times 10^{-3}$ | 1.6 | 16.4 |
| ZTO (70:30) | $5.45 \times 10^{-2}$ | 2.54 | 4.5 | $1.40 \times 10^{-3}$ | 2.41 | 18.4 |
| ZTO (50:50) | $3.69 \times 10^{-2}$ | 3.26 | 5.2 | $1.12 \times 10^{-3}$ | 2.96 | 18.8 |

## Acknowledgements

One of the authors (VJ) is thankful to Mr. Pawan Kulhari, Inter University Accelerator Centre, New Delhi (India) for his kind help in structural experiment, Mr. Devendra Vyas, and Mr. Subodh Srivastava, University of Rajasthan, Jaipur for providing ball milling facility and assistance.

## References

[1] A.J. Freeman, K.R. Poeppelmeirer, T.O. Mason, R.P.H. Chang, T.J. Marks, MRS Bull. 25 (2000) 45.
[2] D.S. Ginley, C. Bright, MRS Bull. 25 (2000) 15.
[3] T. Minami, MRS Bull. 25 (2000) 38.
[4] W.J. Lee, Y.-K. Fang, J.-J. Ho, C.-Y. Chen, L.-H. Chiou, S.-J. Wang, F. Dai, T. Hsieh, R.-Y. Tsai, D. Huang, F.C. Ho, Solid-State Electron. 46 (2002) 477.
[5] K. Ramamoorthy, M. Jayachandran, K. Sankaranarayanan, P. Misra, L.M. Kukreja, C. Sanjeeviraja, Sol. Energy 77 (2004) 193.
[6] K. Momura, H. Ohta, A. Takagi, T. Kamiya, M. Hirano, H. Hosono, Nature 432 (2004) 488.
[7] T. Minami, S. Tsukada, Y. Minamono, T. Miyata, J. Vac. Sci. Technol. A 23 (4) (2005) 1128.
[8] Y. Hayashi, K. Kondo, K. Murai, T. Moriga, I. Nakabayashi, H. Fukumoto, K. Tominaga, Vacuum 74 (2004) 607.
[9] D.L. Young, D.L. Williamson, T.J. Coutts, J. Appl. Phys. 91 (3) (2002) 1464.
[10] X. Wu, T.J. Coutts, W.P. Mulligan, J. Vac. Sci. Technol. A 15 (3) (1997) 1057.
[11] J.H. Ko, I.H. Kim, D. Kim, K.S. Lee, T.S. Lee, J.H. Jeong, B. Cheong, Y.J. Baik, W.M. Kim, Thin Solid Films 494 (2006) 42.
[12] S. Kaleemulla, A. Sivashankar Reddy, S. Uthanna, P. Sreedhara Reddy, Mater. Lett. 61 (2007) 4309.
[13] J.H. Ko, I.H. Kim, D. Kim, K.S. Lee, T.S. Lee, B. Cheong, W.M. Kim, Appl. Surf. Sci. 253 (2007) 7398.
[14] W.J. Moon, J.H. Yu, G.M. Choi, Sens. Actuators B 80 (2001) 21.
[15] X.W. Sun, L.D. Wang, H.S. Kwok, Thin Solid Films 360 (2000) 75.
[16] C.D. Wagner, W.M. Riggs, L.E. Davis, J.F. Mouldar, G.E. Muilenberg, Handbook of X-Ray Photoelectrons Spectroscopy, Perkin Elmer Corporation, Minnesota, 1979.
[17] W. Wohlmuth, I. Adesida, Thin Solid Film 479 (2005) 223.
[18] P.K. Biswas, A. De, L.K. Dua, L. Chkoda, Bull. Mater. Sci. 29 (2006) 323.
[19] T. Ishida, H. Kobayashi, Y. Nakato, J. Appl. Phys. 73 (1993) 4344.
[20] J.C.C. Fan, J.B. Goodenough, J. Appl. Phys. 48 (1977) 3524.
[21] J.H.W. De Witt, J. Solid State Chem. 20 (1977) 143.
[22] G.B. Gon, Z.A. Lez, J.B. Cohen, J.H. Hwang, T.O. Mason, J. Appl. Phys. 89 (2001) 2550.
[23] W.-F. Wu, B.-S. Chiou, Appl. Surf. Sci. 68 (1993) 497.